Polymer dynamics and diffusive properties in ultra-thin photoresist films

Christopher L. Soles[*a], Ronald L. Jones [a], Joseph L. Lenhart [a], Vivek M. Prabhu [a], Wen-Li Wu [a], Eric K. Lin [a], Dario L. Goldfarb [b], Marie Angelopoulos [b]
[a]NIST, Polymers Division Gaithersburg, MD 20899-8541;

[b]IBM T. J. Watson Research CenterYorktown Heights, NY 10598

ABSTRACT

A series of experiments are presented to demonstrate thin film confinement effects on the diffusive properties in poly(tert-butoxycarboxystyrene) (PBOCSt). Bilayer diffusion couple measurements reveal that as the thickness of a PBOCSt film is decreased, the kinetics of the deprotection reaction-front propagation (a process involving both the diffusion and reaction of photochemically activated acidic protons) are dramatically hindered. Incoherent neutron scattering measurements suggest that this retardation can be traced to a suppression of local fast relaxations (200 MHz or faster) native to the PBOCSt polymer. The reduced mobility in the thin PBOCSt films is further confirmed with moisture vapor uptake studies performed on a quartz crystal microbalance (QCM). As the film thickness drops below 500 Å there is a strong reduction in the diffusivity of water in the film. In total, these are the first evidences suggesting that the deviations in lithographic performance with decreasing film thickness observed with the bilayer experiments are due to changes in mobility, not reactivity, within a chemically amplified resist.

Keywords: thin films, diffusion, confinement, neutron scattering, photoacid mobility, moisture transport

1. INTRODUCTION

Diffusion is, and will continue to be, a critical parameter in photolithography. Small molecule diffusion into and through a photoresist film occurs in several stages of the lithography, most notably in both the photoacid transport required to generate the latent image and the dissolution process where an aqueous base or developer penetrates the solid film and removes deprotected photoresist. In the microelectronics industry there is a persistent drive to print increasingly smaller lithographic features. This trend towards miniaturization simultaneously dictates that thickness of the photoresist films must also decrease. There are several reasons for the concomitant reduction of film thickness with feature size. First, there is typically a maximum aspect ratio, height to width on the order of 3:1, beyond which buckling instabilities lead to pattern collapse. The pattern collapse problem therefore dictates that film thickness must also decrease with the minimum feature widths. Likewise, smaller features necessitate a shift to short wavelength UV radiation, i.e., 193 nm and 157 nm. This is problematic as most polymers strongly absorb at these wavelengths. Thinner films are needed to minimize absorption and ensure sufficient illumination throughout the film. To date, the minimum dimensions achievable via chemically amplified photoresists are on the order of 100 nm. These length scales begin to encroach the unperturbed dimensions of the macromolecules that comprise the resist and confinement issues *must* be considered. It is well known that thin film confinement of a polymer affects several of the basic thermo-physical properties [1-3]. It is

imperative to understand if and how thin film confinement affects small molecule transport through a thin photoresist film.

It is understood that segmental molecular motions, either along the backbone or localized to side groups, affect the kinetics of small molecule transport through a polymer [4,5]. Several authors argue that these motions have a gating effect that regulates gas, absorbate, or small molecule transport through the inter-chain regions of amorphous polymers [6-9]. This is of consequence in deep UV lithography where the photochemically generated acidic proton (H^+) diffuses through the resist film and induces multiple chemical reactions. Of course, H^+ mobility is somewhat complicated by the fact that diffusion must couple in to an appropriate counter-ion. Nevertheless, with an approximate diameter of 1 Å, H^+ should readily have access and move within the inter-chain regions of an amorphous polymer. It remains to be seen though how the high frequency local chain motions, such as segmental vibrations, librations, rotations, relaxations, etc., affect H^+ mobility in these inter-chain regions.

We recently demonstrated, using incoherent neutron scattering [10-14], that thin film confinement affects the high-frequency atomic motions in a range of polymers. The collection of atomic and molecular motions faster than 200 MHz are parameterized in terms of their hydrogen-weighted, mean square atomic displacement $\langle u^2 \rangle$. Specifically, we find that thin film confinement leads to a suppression of $\langle u^2 \rangle$, or reduced local mobility on the nanosecond time scale. As $\langle u^2 \rangle$ is less than few $Å^2$ in most solid polymers, the time and length scales of these dynamics are appropriate to influence H^+ mobility and the photolithography process. We tentatively established this correlation by comparing the suppression of the fast relaxations evidenced by neutron scattering to the kinetics of the reaction-diffusion front propagation. Model bilayer diffusion couples [15], where photoacids from a thick feeder layer diffuse into and induce deprotection in a resist underlayer, reveal that the kinetics of reaction-diffusion process decrease as the thickness of the receiving layer (resist) is reduced.

Here we generalize these finding and demonstrate that the diffusion of H_2O into the photoresist film is also kinetically hindered as the thickness of the resist decreases. The kinetics of moisture uptake is tracked through a series of quartz crystal microbalance (QCM) experiments under humid conditions. We find that the suppression in the kinetics of moisture absorption mimics both the retardation of the reaction-diffusion front kinetics and the reduced mobility in $\langle u^2 \rangle$. The parallel variation (with film thickness) of the lithographic bilayer and moisture absorption kinetics is an important distinction since the former involves both reaction and diffusion while the latter is non-reacting, i.e., simple diffusion. This suggests that the deviations in lithographic performance with decreasing film thickness are rooted in reduced mobility, not reactivity, near the surface.

2. METHODOLOGY

2.1 Samples

Experiments were performed on the model 248 nm resist formulation: poly(tert-butoxycarboxystyrene) (PBOCSt) and poly(4-hydroxystyrene) (PHOSt). While this resist will not be utilized for sub-100 nm lithography because of transparency limitations, it is one of the most widely studied and understood resist formulations and therefore suitable for demonstrating general thin film deviations. For the QCM experiments the PHOSt ($M_{n,r}$ = 8,000) was purchased from Triquest [16]. The protected analog was then created by attaching t-butylene 4-vinylphenyl carbonate (Aldrich) onto the 4 position of the phenol ring via free radical polymerization [17]. The chemical structures are identified in Figure 1, along with the simplified reaction scheme whereby the base-insoluble PBOCSt converts into base-soluble PHOSt through the action of the H^+ photoacid. Deprotection consumes the tert-butylcarboxy group, volatilizing it into CO_2 and isobutylene (which leave the sample) and regenerates H^+.

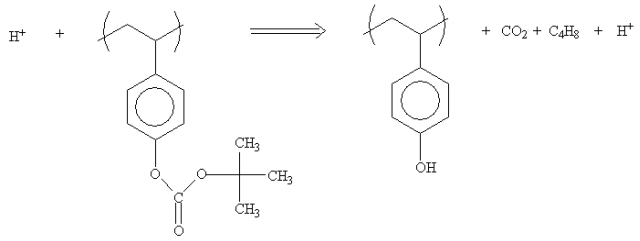

Figure 1. Simplified schematic depicting how PBOCSt reacts with an acidic proton to generate PHOSt, CO_2, isobutylene, and a regenerated acidic proton. This acid then diffuses through the polymer and reacts with another PBOCSt monomer.

The PBOCSt was dissolved in propylene glycol methyl ether acetate (PGMEA) at different mass loadings. The solutions were filtered through a 0.45 μm Teflon filter and spun cast at 2000 rpm onto quartz crystal substrates. The quartz crystals Q-Sense (the QCM manufacturer) were 14 mm in diameter, approximately 0.3 mm thick, and had circular gold electrodes deposited on either side creating an active area in the center of the wafer of approximately 20 mm^2. To mimic the Si wafer substrates in the bilayer and neutron scattering experiments, the quartz crystals were purchased with a thin layer of silicon oxide deposited on top of the gold. The crystals were cleaned prior to spin coating by rinsing with acetone and exposing them for 10 min in a UV-ozone chamber. Excess solvent was removed from the as-cast PBOCSt films with a 2 h post apply bake at 120 °C under a vacuum of 0.1 Pa. We have confirmed that these conditions do not induce significant thermal deprotection.

2.2 Methods

This paper compares the trends in mobility as seen by incoherent neutron scattering, lithographic bilayer diffusion couple, and quartz crystal microbalance experiments. The neutron scattering [14] and bilayer [15] experimental details have been described previously. Briefly, incoherent neutron scattering measurements were performed on the High Flux Backscattering Spectrometer (HFBS) on the NG2 beamline at the NIST Center for Neutron Research [18]. These thin film scattering experiments, performed on a range of polymer films [10-14], record the incoherent elastic scattering intensities, $I_{elastic}$, as a function of Q, where $Q = 4\pi\sin(\theta)/\lambda$, θ being the scattering angle and λ the neutron wavelength. The Q dependence of the elastic scattering is analyzed within the framework of the Debye-Waller approximation. In this context,

$$I_{elastic}(Q) \propto e^{-\frac{1}{3}Q^2\langle u^2\rangle} \qquad (1)$$

where $\langle u^2\rangle$ denotes the hydrogen weighted mean-square atomic displacement. Within this approximation $\langle u^2\rangle$ is defined by the linear slope of $ln(I_{elastic}(Q))$ vs. Q^2. As the thermal motions are excited, there is a decrease in the intensity of the elastically scattered neutrons and correspondingly an increase in $\langle u^2\rangle$. This is analogous to the thermal decrease in intensity and broadening of an X-ray diffraction peak in a crystalline material. These are not truly inelastic neutron scattering measurements, so we are not able to precisely quantify the time scale of the dynamics. However, the 0.85 μeV energy resolution of the spectrometer means that only motions faster than 200 MHz lead to an increase of $\langle u^2\rangle$; slower motions appear as elastic scattering.

The bilayer lithographic diffusion experiments are described in detail elsewhere [15]. Briefly, PBOCSt films of varying thickness are spin cast from PGMEA onto hydrophobic Si wafers and post apply baked at 130 °C for 60 s to remove residual solvents. Then, a thick PHOSt film is spin cast on top of the PBOCSt film from butanol (butanol does not dissolve PBOCSt), creating a bilayer structure. The photoacid generator, di(t-butylphenyl) iodonium perfluorooctanesulfanate (PFOS), is added to the PHOSt layer at 5 % by mass loading so that photoacids are only created (upon UV illumination) in the top half of the diffusion couple. Then, upon heating the photoacids diffuse into the lower layer and induce deprotection, turning the PBOCSt into PHOSt. Only the PHOSt is removed upon dissolution and the extent of the reaction front propagation can be determined from the change in the thickness of the original PHOSt underlayer. By performing these experiments as a function of baking time, we extract an effective diffusion coefficient for the reaction front propagation kinetics.

The quartz crystal microbalance experiments were performed on a Q-Sense instrument, which drives the crystal at a primary frequency of 5 MHz. Unlike traditional QCMs, Q-Sense pulses the crystal and monitors both the resonant frequency and the damping of the vibration. In these experiments we only utilize the resonance peak shifts. In addition to the primary frequency of 5 MHz, data are simultaneously collected for the overtones at 15 MHz, 25 MHz, and 35 MHz. The sample preparation protocol for the QCM measurements consisted of removing excess solvent from the as-cast PBOCSt film for 2 h at 120 °C under a vacuum of 0.10 Pa. Once the films were removed from the vacuum, they were immediately mounted in the QCM apparatus, with sample temperature set to 27 °C. The films were then purged with dry air for two to three hours while the resonance signal equilibrated. Once a stable resonance signal was achieved, the dry air stream was diverted through a bubbler containing deionized water at room temperature (approximately 22 °C to 24 °C). This saturated the air to a relative humidity of approximately 100%, which was purged through the QCM. As water diffuses into the film the mass uptake induces a shift in the resonant frequency. The flow of moist air across the sample continued until the frequency shift stabilized, at which point equilibrium is assumed.

3. RESULTS

Figure 2 summarizes the effective reaction-diffusion coefficients obtained from the bilayer experiments discussed earlier [15]. These measurements, performed at 110 °C, indicate that the kinetics of the reaction front propagation are hindered when the PBOCSt layer becomes thinner, especially for films less than 500 Å. It is crucial to realize that these diffusion coefficients reflect a complicated balance of chemical kinetics and diffusion. A photoacid (H^+) must diffuses

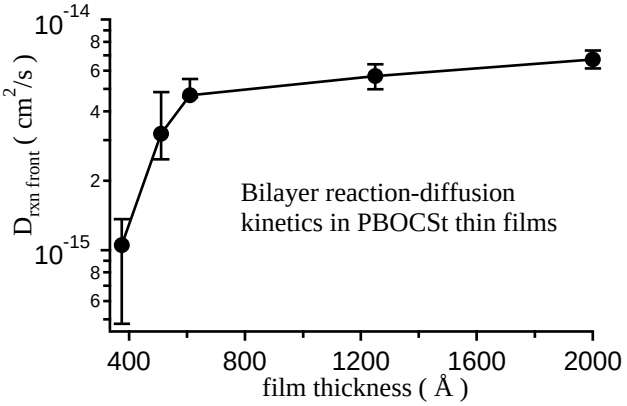

Figure 2. Effective diffusion coefficients as a function of the PBOCSt film thickness for the reaction-diffusion bilayer experiments described in reference [15]. Error bars indicate the standard uncertainty in the effective diffusion coefficients.

through the resist and find a reactive protecting group. This regenerates an acidic proton, which diffuses to the next protecting group, and henceforth sets up a reaction-diffusion cycle. It is not immediately apparent at this point if the retardation of the reaction front kinetics is due to changes in the diffusive properties or mobility within the polymer film, or more fundamentally related to the chemical kinetics of the reaction itself. Nevertheless, it is apparent that the lithographic performance of the resist is compromised by the state of thin film confinement.

To understand how the mobility of the polymer itself is affected by confinement, we turn to incoherent neutron scattering. Neutrons are scattered directly by the atomic nuclei and therefore unambiguously reflect the dynamics of the polymer. As shown in Figure 3, the amplitude of the fast atomic relaxations (faster than 200 MHz) is suppressed by thin film confinement. As the thickness of the PBOCSt film decreases there is a clear and precipitous decrease of $\langle u^2 \rangle$. It is not clear if this represents a slowing of the motions to frequencies below 200 MHz or an actual decrease in the amplitude of the motion; both scenarios would have the same effect. Regardless, from a transport perspective both possibilities (decreased jump length or jump frequency) point to a decreased diffusion coefficient. We provided [14] heuristic arguments, based on empirical exponential correlations of viscosity and the inverse of $\langle u^2 \rangle$ ($\eta \sim exp(1/\langle u^2 \rangle)$), that the reduction of $\langle u^2 \rangle$ is consistent with reduced diffusion in the thin PBOCSt films. This follows since diffusivity typically varies inversely with viscosity ($D \sim 1/\eta$). Using these arguments we demonstrated that length-scales at which the

confinement effects are felt in both the neutron scattering and bilayer experiments were the same [14]. This suggests that thin film deviations in lithographic performance are related to the dynamics of the polymer.

The moisture absorption experiments in the thin PBOCSt films are useful because they reveal thin film changes in the diffusive properties for a non-reacting small molecule penetrant. This is needed to separate the chemistry and mobility effects from the observed deviations in lithographic performance from the bilayer experiments. Note that the physical diameter of a water molecule (approximately 3 Å) is, to a first approximation, comparable to an acidic proton (approximately 1 Å). From this perspective using H_2O diffusion to understand H^+ dynamics is a reasonable extension; the length-scales for confinement deviations should be similar.

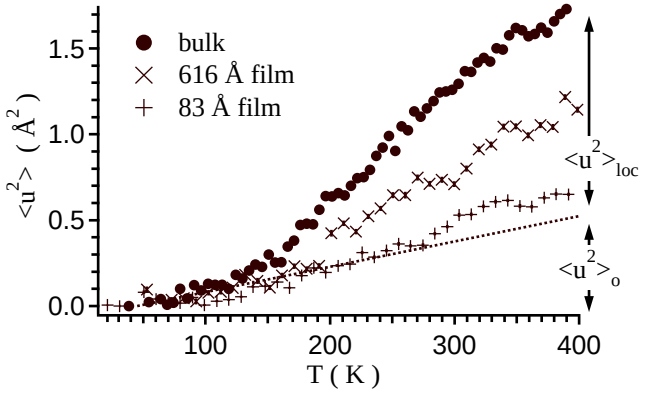

Figure 3. The thermal dependence of the mean-square atomic displacements, $\langle u^2 \rangle$, are shown as function of thickness for the PBOCSt films. Reducing film thickness suppresses $\langle u^2 \rangle$ as described in detail elsewhere [14]. The standard uncertainty in determining $\langle u^2 \rangle$ is comparable to the size of the data markers.

Figure 4 displays representative raw data for a QCM moisture absorption experiment. In this example the third overtone (15 MHz) of the 5 MHz resonant frequency is plotted as a function of time. There are several features of this curve warranting further discussion. After the initial mounting of the crystal, the signal goes through a transient period of approximately 1 h before the frequency stabilizes as the cell comes into thermal equilibration. Once the transient stabilizes, the resonant frequency displays a slight linear drift (emphasized in the main portion of Figure 4). Ideally, a film neither gaining nor losing mass should produce a flat signal without this drift in the resonance. This *should* be the case here since the dry film (taken directly from the vacuum oven) is purged with dry air. However there appears to be a gentle increase in the resonant frequency, which seems to indicate a mass loss. Recall, for a harmonic oscillator, $\omega^2 = k/m$ where ω is the resonance frequency, k is the spring constant, and m is the mass; an increase in ω indicates a decrease in m.

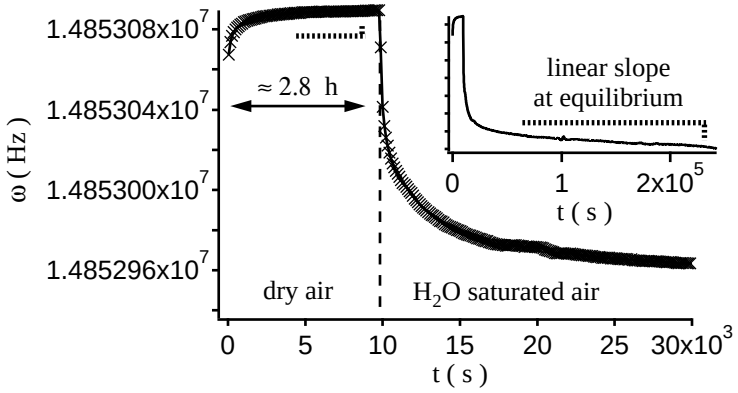

Figure 4. Typical QCM frequency shift data is shown for 3rd overtone of the resonant frequency in both dry and moisture saturated air. The inset, whose vertical axis is the same as the main part of the figure, extends the data to very long times to demonstrate the linear drift in the signal at equilibrium. The accuracy to which ω is determined is better than 0.1 Hz.

Midway through Figure 4 the resonance frequency exhibits a rapid decrease. This corresponds to the time t at which the purge is switched from dry to moisture-saturated air. The decrease in frequency indicates the increase in the mass as water absorbs into the film. The rate of uptake (decrease in frequency) slows at longer times, in the expected diffusive manner. At long times though, this diffusive process does not plateau (see inset of Figure 4); once again there is slight linear drift in the resonance signal. In this particular case the slope of the drift is positive for the dry air and negative for the moisture-saturated air. However, both *positive* and *negative* slopes have been observed for both the dry and moisture-saturated environments. At this time we are unable to identify the origins of this signal drift. We believe that this is inherent to the electronics that control the QCM since we have extensively explored the relevant variables. More importantly, we have determined that drift is not the result of a slow adsorption/ desorption of small molecules onto the surface of the film. The drift is present irrespective of the polymer and similar drifts occur on uncoated or blank quartz crystals. Furthermore, we have enclosed the entire QCM apparatus in a vacuum (approximately 0.1 Pa) and find that the slope of the drift does not depend upon the environment. Comparable negative slopes were observed in both air and the vacuum. It is highly unlikely that the film gains mass in the vacuum, especially at the same rate as in the air. While we are unable to account for this linear signal drift, it does not appear to be related to the moisture uptake problem at hand. Therefore we assume that extended linear variations with time of the resonance frequency are an indication of equilibration.

To extract diffusion coefficients from the raw frequency shift data, we adapt the following procedure. First, we define time $t = 0$ to coincide with the initial drop in frequency that occurs when the film is first exposed to the moisture saturated air. Then we look at long times, where the frequency evolution is linear, and determine a slope constant, S, for the linear drift. By subtracting $t*S$ from each data point we obtain frequency shift data that plateaus at long times, as expected for a diffusive process. The frequency shifts ($\Delta\omega$) are then converted into mass uptakes (Δm) through the Saurbrey equation [19]:

$$\Delta\omega = (-n/C)\,\Delta m \qquad (2)$$

where n is the overtone (1 for 5 MHz; 3 for 15 MHz; 5 for 25 MHz; 7 for 35 MHz) and C is a characteristic constant for the crystal. For the crystal manufactured by Q-Sense, C is 17.7 ng cm^{-2} Hz^{-1}.

Figure 5 displays a typical moisture uptake curve in a diffusive format, i.e., Δm versus ($t^{1/2}/h$) where h is the sample thickness (in Å). In this representation, the short-time Fickean approximation [4] can be used to extract a diffusion coefficient from the initial slope (linear fit indicated) and the equilibrium uptake. The data displayed in Figure 5 is for a relatively thick (3500 Å) PHOSt film and the corresponding diffusion coefficient is 1×10^{-13} cm^2/sec. Fickean diffusion is, however, a simplification of the process. This is readily seen from the Fickean profile regenerated from the estimated diffusion coefficient and equilibrium uptake (dashed line). The fit marginally parameterizes the data in the region of where the uptake rolls over into the equilibrium plateau. Nevertheless, the short-time Fickean approximation provides an order of magnitude estimate of the diffusion coefficient.

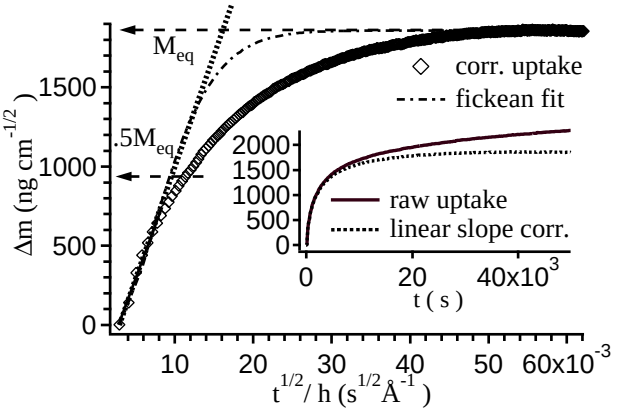

Figure 5. The mass of water absorbed/adsorbed for a 3500 Å PHOSt film is displayed in a Fickean format (root time divided by thickness). The heavy dashed line indicates the initial slope used to estimate the diffusion coefficient from the short-time Fickean approximation and the equilibrium uptake M_{eq}. Also indicated is the corresponding Fickean profile (dot-dashed line). The inset displays the same uptake data as a linear function of time, emphasizing how the linear slope correction at long times affects the data. The accuracy in which Δm can be measured is much greater than the size of the data markers.

Figure 6 displays how the effective moisture diffusion coefficient varies as a function of the PBOCSt film thickness. Like the reaction front propagation kinetics, there is a strong decrease in the effective diffusion coefficient of water as the film thickness decreases. As mentioned previously, in addition to the primary 5 MHz frequency, the QCM simultaneously collects data for the overtones at 15 MHz, 25 MHz, and 35 MHz. These overtones can be analyzed in a similar manner and the diffusion coefficients in Figure 5 represent an average of the 4 data sets, with the error bars

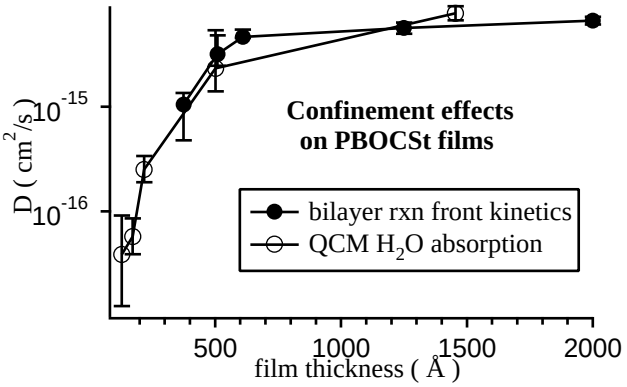

Figure 6. The effective diffusion coefficients from the bilayer reaction front experiments [15] are directly compared to the moisture absorption diffusion coefficients from the QCM experiments. Both measurements show the same deviations with decreasing PBOCSt film thickness. The error bars for the bilayer experiments indicate standard uncertainties while for the QCM experiments the error bars indicate the range of data points determined from the 4 modes of the resonance frequency (see text).

indicating the range or spread. From the relatively small spreads one can see that all 4 data sets are typically consistent. We have performed multiple measurements of the thinnest films and also find that the run-to-run repeatability is also very good. We do not have sufficient data to quote a standard deviation in the diffusion coefficient, but it appears that the variations with film thickness will be greater than the anticipated standard uncertainty.

4. DISCUSSION

Note that the estimated diffusion coefficients for the thickest films are nominally one to two orders of magnitude smaller than expected; diffusivities in the range of 1×10^{-8} cm^2/sec to 1×10^{-11} cm^2/sec are common for moisture diffusion in bulk,

glassy polymer at room temperature [4,20-22]. D in the thickest PBOCSt film (1500 Å, or 0.15 μm) in Figure 6 is about 1×10^{-14} cm^2/sec and should be approaching a bulk-like value. From the trend it looks as if the diffusivities will continue to increase slightly as film thickness increases, approaching to within an order of magnitude of the conventional bulk-like diffusivity range. To a first approximation, it appears if our experiments are producing reasonable data, even in light of the problems with the sloping background. An order of magnitude agreement is also reasonable given the simplifications implicit in the Fickean approximation. For now we emphasize changes in the diffusivity with film thickness. Shortcomings of the Fickean model or the sloping background correction are equally applicable for all films meaning that the changes with film thickness are robust. It is important to note that the equilibrium uptake values are consistent with complementary swelling data (not presented here). The thickness of similar films was measured with X-ray reflectivity and the equilibrium uptakes estimated from the increase in thickness and the QCM uptakes are consistent, lending further credence to the QCM data.

When the film thickness approaches 100 Å, the D's are on the order of 1×10^{-17} cm^2/s. This is extremely slow for moisture diffusion into a polymer and therefore cause for concern. D's of 1×10^{-17} cm^2/s are appropriate for processes involving molecular reorganization of polymer chains, clearly an intriguing notion for our thinnest films. To the best of our knowledge there have been few, if any, diffusion studies on such thin polymer films. There are several QCM moisture absorption studies on thicker films (100's of nm), reporting D's on the order of 1×10^{-6} cm^2/s to 1×10^{-12} cm^2/s [23-26]. These values seem reasonable since they are largely consistent with moisture diffusion in bulk polymer as well as our thicker films. However, we emphasize that most of these examples use a relatively "soft" post apply bake (a few min in air at an elevated temperature well below the ultimate T_g of the material) to remove the residual solvent that plasticizes the film and enhances transport. In our studies we used a "hard" bake (120 °C in vacuum for 2 h) to remove greater fractions of the casting solvent. This leads to reduced diffusivity in our thin films and might account for why our D's in the thicker films lie at the lower end of the range for typical bulk diffusivities discussed above.

A possible source of error in our diffusivities stems from that fact that we do not account for moisture adsorption (not absorption). A small layer of water will adsorb onto the surface of the film, which in a thin films can become an increasingly significant fraction of the total adsorbed/absorbed moisture. It is difficult to accurately correct for this effect, but our preliminary estimates indicate that adsorption errors, which overestimate the equilibrium uptake, could lead to diffusivities in our thinnest films that are underestimated by about an order of magnitude. These estimates come from adsorption studies onto blank QCM crystals where absorption is absent. Of course, the adsorption behavior will be affected the different surface energies of the polymer and the quartz crystal. However, the hydrophilic SiO_x surface of the QCM crystal would seemingly be more prone to adsorption than the more hydrophobic polymer. The order of magnitude increase is probably an upper bound on the uncertainty in D, and clearly smaller that the variations we observe with film thickness (nearly 4 orders of magnitude). In this respect, the variations in D with film thickness are probably real and reasonable. To clarify this issue, we are preparing neutron reflectivity studies with deuterated water vapor to experimentally measure the thickness of the adsorbed water layer.

The extremely small diffusion coefficient and notion of water-induced structural reorganization in the thinnest films is intriguing. When the film thickness is on the order of 50 Å to 100 Å, it is likely that the chains lie flat along the surface, giving up entropy for enhanced packing as dictated by the confining walls. If the packing is enhanced in the thin film, it is plausible that the diffusivity decreases dramatically. There are bulk studies that clearly demonstrate a strong decreases in the diffusivity of moisture as the Van der Waals packing volume increases in both polyimides [27] and epoxies [28]. Likewise, we observe a decrease in the low temperature diffusivity of moisture with a decrease in the unoccupied volume fraction evidenced by positron annihilation lifetime spectroscopy [22]. This generally reflects the notion that small molecules diffuse slower through tightly packed media. If the state of thin film confinement enhances packing, hindered diffusion would be the natural consequence. This picture is reasonable given the experimental evidence for a dynamically dead layer (retarded mobility) at the interface of a polymer and a rigid substrate [29-33]. Then, when water diffuses into these thin films, mobility is enhanced due to the plasticization effect. It seems plausible that with enhanced mobility, the highly constrained films would relax and try to regain entropy by swelling with water. This might explain why the diffusion coefficients are consistent with polymer chain motions; the chains are reorganizing in response to the moisture. In this respect the role of moisture is similar to a solvent that can really affect the chain movement and structure. There are studies of solvent absorption/desorption in both photoresists [34] and polystyrene [35] that report diffusion coefficients on the order of 1×10^{-14} cm^2/s to 1×10^{-20} cm^2/s, encompassing the values reported herein. This is an

important distinction to make since for most polymer glasses, moisture diffusion can be modeled as a pentrant hopping through a rigid matrix. However, in the case of the solvent the matrix is not rigid and chains must reorganize. When there is very little solvent present, like the small amounts of water absorbed into the PBOCSt film, this reorganization is would be very slow. This is an intriguing notion, but it remains to be verified if a moisture-induced structural reorganization is responsible for the slow absorption kinetics in our thinnest films.

Returning to the bilayer experiments, Figure 6 includes the effective reaction front diffusion coefficients reported in Figure 1. It is striking that the reaction front and moisture absorption display nearly identical effective diffusion coefficients, including the trend of decreasing kinetics with decreasing film thickness. This clearly supports the rather slow effective diffusion coefficients extracted from the QCM data. Likewise, the PBOCSt mobility estimates derived from $\langle u^2 \rangle$ also support this notion that the diffusive properties in a thin film are strongly retarded with decreasing film thickness. This is an important distinction to make since it suggests that the deviations in the lithographic performance evidence in the bilayer experiments can be traced to changes in the diffusivity, not reactivity. The reaction front experiments reflect a complicated balance of reaction and diffusion. The fact that water, a non-reacting penetrant, also shows the same kinetic trends is strong evidence that the observations are due to changes in the thin film diffusivity.

To emphasize this last point, we plot the ratio of the bulk to thin film diffusion coefficients as a function of film thickness for the three different experiments discussed herein. A similar plot was produced in our recent publication with just two of the data sets, demonstrating that the $\langle u^2 \rangle$ predictions were consistent with the bilayer experiments. To estimate a bulk moisture diffusion coefficient from the QCM experiments, we note that a plot $ln\ (D_{QCM})$ versus $1/h$ is linear, similar to analogous plots used to parameterize T_g depressions in the thin polymer film literature [1-3]. In this representation the linear intercept at $1/h = 0$ provides an estimate of 1.11×10^{-14} cm^2/s for the diffusion coefficient in an infinitely thick film (bulk). Using this value for the bulk diffusion coefficient of water in PBOCSt, Figure 6 compares D_{bulk} / D_{film} as a function of h for all three data sets. The agreement is excellent and all three phenomena show thin film deviations at similar length scales. This suggests that inherent reductions in the polymer mobility as the film thickness

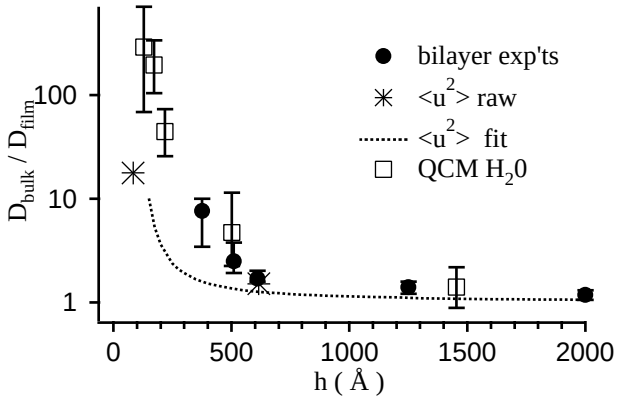

Figure 7. The ratio of the bulk to film diffusion coefficients are displayed as a function of film thickness for the bilayer, neutron scattering, and QCM experiments described in the text. All three techniques indicate similar reductions of mobility at similar length scales. The error bars are a simple propagation of the uncertainties presented in the previous figures.

decreases also retards the small molecule diffusion within thin film. This reduced diffusion affects the lithographic performance in terms of a dramatic slowing of the reaction front propagation. The length scales at which these confinement effects become significant appear to be on the order of 500 Å. Given these dimensions, a similar mechanism might be related to either the “footing” and/or “scumming” effects that are often observed in commercial resist formulations. These effects occur immediately adjacent to the rigid substrate where similar reductions of mobility would be anticipated. Current research efforts in our lab are dedicated to exploring this possibility in greater detail.

5. CONCLUSIONS

To summarize, we have studied the dynamics in thin PBOCSt films by three independent techniques. Bilayer diffusion couple experiments show that the kinetics of the reaction front propagation whereby PBOCSt turns into PHOSt under the action of a photochemically generated acidic proton is dramatically retarded as the thickness of the PBOCSt film is decreased. Likewise, the inherent atomic/molecular mobility in PBOCSt measured with incoherent neutron scattering is also diminished at similar length-scales of thin film confinement. The effect is further generalized through observations that the diffusion of water into the PBOCSt film shows the same kinetic deviations (retardation) with decreasing film thickness as the reaction front rate and the polymer mobility. In all three instances, the reduced mobility in the PBOCSt films becomes significant when the film thickness drops below 500 Å. These correlations empirically *suggest* that the deviation in the lithographic performance in the bilayer experiments is due to changes in the mobility within the PBOCSt film and not necessarily the chemical reactivity.

ACKNOWLEDGEMENTS

Funding for this work comes from the DARPA Advanced Lithography Program, grant N66001-00-C-8083. The neutron scattering activities are made possible in part by the National Science Foundation, under Agreement No. DMR-0086210. Support for Ron Jones and Vivek Prabhu comes from the National Research Council NIST Postdoctoral Fellowship Program. The authors would like to further thank Rob Dimeo, Dan Neumann, and Bryan Vogt for their valuable discussions and review of the manuscript.

REFERENCES

1. R. A. L. Jones, R. W. Richards, *Polymers at Surfaces and Interfaces*, Cambridge University Press, Cambridge, UK (1999)
2. A. Karim and S. Kumar, *Polymer Surfaces, Interfaces, and Thin Films*, World Scientific, Singapore (1999)
3. R. A. L. Jones, *Curr. Opinions in Colloid & Interf. Sci.* **4**, 153 (1999)
4. J. Crank and G. S. Park, *Diffusion in Polymers*, Academic Press, London (1968)
5. P. Neogi, *Diffusion in Polymers*, Marcel Dekker, Inc., New York (1996)
6. L. G. F. Stuk, *J. Polym. Sci. B* **28**, 127 (1990)
7. M.-B. Haag, W. J. Koros, J. C. Schmidhauser, *J. Polym. Sci. B* **32**, 1625 (1994)
8. M. Ponitsch, P. Gotthardt, A Gruger, H. G. Brion, R. Kirchheim, *J. Polym. Sci. B* **35**, 2397 (1997)
9. C. L. Soles and A. F. Yee, *J. Polym. Sci. B* **38**, 792 (2000)
10. C. L. Soles, J. F. Douglas, W.-l. Wu, R. M. Dimeo, *Phys. Rev. Lett.* **88**, 037401 (2002)
11. C. L. Soles, E. K. Lin, J. L. Lenhart, R. L. Jones, W.-l. Wu, D. L. Goldfarb, M. Angelopoulos, *J. Vac. Sci. Technol. B* **19**, 2690 (2001)
12. C. L. Soles, J. F. Douglas, W.-l. Wu, H. Peng, D. W. Gidley, *Mat. Res. Soc. Symp. Proc.* **710**, DD3.7.1 (2002).
13. C. L. Soles, J. F. Douglas, W.-l. Wu, R. M. Dimeo, *Macromolecules* **36**, 373 (2002)
14. C. L. Soles, J. F. Douglas, E. K. Lin, J. L. Lenhart, R. L. Jones, W.-l. Wu, D. L. Goldfarb, M. Angelopoulos, *J. Appl. Phys.* **93**, 1978 (2003)
15. D. L. Goldfarb, M. Angelopoulos, E. K. Lin, R. L. Jones, C. L. Soles, J. L. Lenhart, W.-l. Wu, *J. Vac. Sci. Technol. B* **19**, 2699 (2001)
16. Certain commercial equipment and materials are identified in this paper in order to specify adequately the experimental procedure. In no case does such identification imply recommendation by the National Institute of Standards and Technology nor does it imply that the material or equipment identified is necessarily the best available for this purpose.
17. J. M. Frechet, E. Eichler, H. Ito, and C. G. Willson, *Polymer* **24**, 995 (1983)
18. P. M. Gehring and D. A. Neumann, *Physica B* **241-243**, 64 (1998)
19. G. Sauerbrey, *Z. Phys.* **155**, 206 (1959)
20. P. Neogi, *Diffusion in Polymers*, Marcel Dekker, New York (1996)
21. W. R. Vieth, *Diffusion in and Through Polymers*, Hanser Publishers, New York (1991).
22. C. L. Soles, F. T. Chang, D.W. Gidley, A. F. Yee *J. Polym. Sci.: Part B: Polym. Phys.* **38**, 776 (2000).
23. D. K. Yang, W. J. Koros, H. Hopfenberg, V. Stannett *J. Appl. Polym. Sci.* **30**, 1035 (1985).
24. D. K. Yang, W. J. Koros, H. Hopfenberg, V. Stannett *J. Appl. Polym. Sci.* **31**, 1619 (1986)

25. K. Okamoto, N. Tamihara, H. Wantanabe, K. Tanaka, H. Kita, A. Nakamura, K. Nakagawa *J. Polym. Sci.: Part B: Polym. Phys*. **30**, 1223 (1992)
26. W.-L. Chen, K. R. Shull, T. Papatheodorou, D. A. Styrkas, J. L. Keddie *Macromolecules* **32**, 136 (1999).
27. S. Numata, K. Fujisaki, N. Kinjo *Polymer* **28**, 2282 (1987)
28. V. Bellenger, J. Verdu, E. Morel *J. Mater. Sci*. **24**, 63 (1989)
29. G. B. DeMaggio, W. E. Frieze, D. W. Gidley, M. Zhu, H. A. Hristov, A. F. Yee, *Phys. Rev. Lett*. **78**, 1524 (1997)
30. W. E. Wallace, J. H. Van Zanten, W.-l. Wu, *Phys. Rev. E* **52**, R3329 (1995)
31. D. J Pochan, E. K. Lin, S. K. Satija, W.-l. Wu, *Macromolecules* **34**, 3041 (2001)
32. J. H. Van Zanten, W. E. Wallace, W.-l. Wu, *Phys. Rev. E* **53**, R2053 (1996)
33. D. W. Gidley, G. B. DeMaggio, W. E. Frieze, M. Zhu, H. A. Hristov, A. F. Yee, *Mat. Sci. Forum* **255-257**, 635 (1997)
34. C. A. Mack, K. E. Mueller, A. B. Gardiner, J. P. Sagan, R. R. Dammel, C. G. Willson J. Vac. Sci. Technol. B 16, 3779 (1998)
35. N. E. Filioppov, J. Colloid Interface Sci. 212, 589 (1999)